Mater. Res. Soc. Symp. Proc. Vol. 1324 © 2011 Materials Research Society
DOI: 10.1557/opl.2011.1056

AlGaN Channel HEMT with Extremely High Breakdown Voltage

Takuma Nanjo[1], Misaichi Takeuchi[2], Akifumi Imai[1], Yousuke Suzuki[1], Muneyoshi Suita[1], Katsuomi Shiozawa[1], Yuji Abe[1], Eiji Yagyu[1], Kiichi Yoshiara[1] and Yoshinobu Aoyagi[2]
[1]Mitsubishi Electric Corporation, Advanced Technology R & D Center, 8-1-1, Tsukaguchi-honmachi, Amagasaki, Hyogo 661-8661, JAPAN
[2]Ritsumeikan Global Innovation Research Organization, Ritsumeikan University, 1-1-1 Noji-Higashi, Kusatsu, Shiga 525-8577, JAPAN

ABSTRACT

A channel layer substitution of a wider bandgap AlGaN for a conventional GaN in high electron mobility transistors (HEMTs) is an effective method of enhancing the breakdown voltage. Wider bandgap AlGaN, however, should also increase the ohmic contact resistance. Si ion implantation doping technique was utilized to achieve sufficiently low resistive source/drain contacts. The fabricated AlGaN channel HEMTs with the field plate structure demonstrated good pinch-off operation with sufficiently high drain current density of 0.5 A/mm without noticeable current collapse. The obtained maximum breakdown voltages was 1700 V in the AlGaN channel HEMT with the gate-drain distance of 10 μm. These remarkable results indicate that AlGaN channel HEMTs could become future strong candidates for not only high-frequency devices such as low noise amplifiers but also high-power devices such as switching applications.

INTRODUCTION

GaN-based wide bandgap semiconductors have superior electrical properties such as a high electron saturation velocity and a high breakdown field. In particular AlGaN/GaN high-electron mobility transistors (HEMTs) with high-density two-dimensional electron gas have been widely studied for high-power and high-frequency applications.[1-10] To increase a power density of HEMTs, it is a simple strategy to increase a breakdown voltage. Therefore applying a wider bandgap material for a channel layer, which generally enhances the breakdown field (E_c), is one of effective methods. Higher Al composition AlGaN is an available material to increase the breakdown voltage without decreasing a drain current density, because the E_c of AlN, which has about twice wide of the energy bandgap comparing to that of GaN, is about four times larger than that of GaN, and the electron saturation velocity of AlN is almost as same as that of GaN as shown in table I. Although the AlGaN channel HEMTs have high potential to increase the breakdown voltage, the wider bandgap leads to the difficulty to form a sufficiently low resistive ohmic contact. Therefore a breakthrough technology to reduce the contact resistance is required. In order to solve this problem, we employed Si ion implantation doping technique that we have developed for conventional GaN channel HEMTs.[11]

In this paper, we report that AlGaN channel HEMTs, where we utilized Si ion implantation doping technique to achieve sufficiently low resistive contacts, were operated with remarkably enhanced breakdown voltage and sufficiently high drain current density without noticeable current collapse.

Table I. Properties of semiconductor materials using HEMTs

	GaAs	GaN	AlN
Bandgap, E_g (eV)	1.42	3.4	6.2
Electric Breakdown Field, E_c (V/cm)	0.4×10^6	3.3×10^6	12×10^6
Electron Mobility, μ (cm^2/Vs)	8500	2000	1090
Electron Saturation Velocity, V_{sat} (cm/s)	2.0×10^7	2.5×10^7	2.2×10^7
Johnson's figure of merit	7	760	7800
Baliga's figure of merit	9	39	67

EXPERIMENT

Figure 1 shows a cross-sectional structure of fabricated $Al_yGa_{1-y}N/Al_xGa_{1-x}N$ HEMTs. Unintentionally doped epitaxial layers were grown by metalorganic chemical vapor deposition. We prepared three types of $Al_yGa_{1-y}N/Al_xGa_{1-x}N$ heteroepitaxial wafers. As shown in Table II, these were one GaN channel structure on Sapphire substrate and two AlGaN channel structures on Sapphire and SiC substrates, respectively. A barrier layer thickness and a difference of Al composition between the barrier and the channel layer were equivalent in three wafers.

Figure 2 shows a fabrication process of the $Al_yGa_{1-y}N/Al_xGa_{1-x}N$ HEMTs. The fabrication process started with selective Si ions implantation into source/drain regions. ^{28}Si ions were implanted with an energy of 50 keV at a dose concentration of 1 x 10^{15} cm^{-2} at room temperature, and subsequently implanted Si ions were activated by rapid thermal annealing at 1200 ^OC for 5 min in an environment of flowing nitrogen. During the Si ions implantation and the activation annealing, wafer surfaces were capped by 30 nm thick of SiN layer deposited by plasma-enhanced chemical vapor deposition. After removing the SiN cap layer in a HF solution, source/drain ohmic contacts were formed by Ti/Al metallization and subsequent rapid thermal annealing at 600 ^OC for 2 min in an environment of flowing nitrogen. Then device isolation was performed by Zn ion implantation[12] and Ni/Au Schottky gate contact was formed. The fabrication of HEMTs was completed by depositing a SiN dielectric film using catalytic chemical vapor deposition[13-15] and subsequent formation of a Ni/Au field plate which was connected to the gate contact at an electrode pad. All electrodes were defined by a conventional photolithography and liftoff technique, and the all metals were deposited by an electron beam evaporation system. In fabricated $Al_yGa_{1-y}N/Al_xGa_{1-x}N$ HEMTs, the gate length (L_g), the gate width (W_g), the distance between the source and gate (L_{sg}), and the distance between the gate and drain (L_{gd}) were 1, 50, 1, and 2~10 μm, respectively.

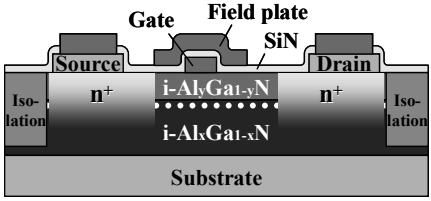

Figure 1. Schematically illustrated cross-sectional view of fabricated $Al_yGa_{1-y}N/Al_xGa_{1-x}N$ HEMTs.

Table II. RMS values, sheet carrier concentrations, electron mobilities, and sheet resistances for three $Al_yGa_{1-y}N/Al_xGa_{1-x}N$ heterostructures.

Barrier layer	$Al_{0.25}Ga_{0.75}N$	$Al_{0.40}Ga_{0.60}N$	$Al_{0.40}Ga_{0.60}N$
Barrier layer thickness (nm)	25	25	25
Channel layer	GaN	$Al_{0.15}Ga_{0.85}N$	$Al_{0.15}Ga_{0.85}N$
Substrate	Sapphire	Sapphire	4H-SiC
RMS (nm)	0.26	0.68	0.41
Sheet carrier concentration (cm^{-2})	8.7×10^{12}	7.9×10^{12}	9.4×10^{12}
Electron mobility (cm^2/Vs)	1550	460	510
Sheet resistance (Ω/sq)	460	1720	1310

- **Epitaxial layer growth**
  i-$Al_yGa_{1-y}N$/ i-$Al_xGa_{1-x}N$ hetero structure
- **Source/Drain Ohmic contact**
  Si ion implantation
  Activation annealing
  Ohmic metal (Ti/Al) deposition
  Alloying annealing
- **Device Isolation**
  Zn ion implantation
- **Gate Schottky contact**
  Schottky metal (Ni/Au) deposition
- **Field plate**
  Dielectric film (SiN) deposition
  Field plate metal (Ni/Au) deposition

Figure 2. Fabrication process of $Al_yGa_{1-y}N/Al_xGa_{1-x}N$ HEMTs.

RESULTS AND DISCUSSION

Eptaxial layer characteristics

Sheet carrier concentrations, electron mobilities and sheet resistances of the three wafers were evaluated from a Hall measurements at room temperature as summarized in Table II. The sheet carrier concentration was decreased by increasing the Al composition in epitaxial layers and increased by substituting the substrate to SiC, which were attributed to crystal quality degradation by increasing the Al composition and improvement by substituting the substrate to SiC mainly due to less lattice mismatch with the substrate. As proof of the alteration in crystal quality, a surface morphology and a RMS value from AFM images were degraded by increasing the Al composition and improved by substitution of the substrate to SiC as shown Fig. 2 and table II. Electron mobility was also decreased by increasing the Al composition in epitaxial layers which was attributed to an increase of alloy scattering and this degradation is one of disadvantages in AlGaN channel HEMTs in presence. The electron mobility in AlGaN channel structure, however, was higher than the calculated value[16] and it was improved by substituting the substrate to SiC due to the improvement in crystal quality. The obtained sheet resistances were sufficiently low to operate the HEMTs.

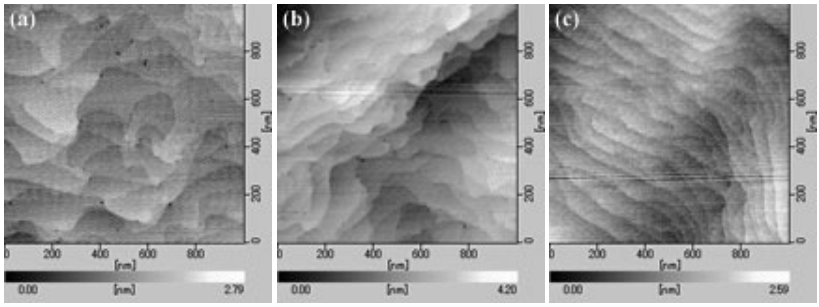

Figure 3. AFM images of (a) $Al_{0.25}Ga_{0.75}N/GaN$ layers on Sapphire substrate, (b) $Al_{0.40}Ga_{0.60}N/Al_{0.15}Ga_{0.85}N$ layers on Sapphire substrate and (c) $Al_{0.40}Ga_{0.60}N/Al_{0.15}Ga_{0.85}N$ layers on SiC substrate.

Ohmic characteristics

Figure 4 shows current-voltage (I-V) curves between two ohmic electrodes spaced 4μm with and without Si ion implantation which were formed on the $Al_{0.40}Ga_{0.60}N/Al_{0.15}Ga_{0.85}N$ epitaxial layers on SiC substrate. In the sample without Si ion implantation, a contact resistance was so high that we could not calculate it from a circular transfer length method (CTLM), because the AlGaN barrier layer was not only unintentionally doped but also the Al composition was higher comparing to the conventional barrier layer of AlGaN/GaN structure. On the other hand, in the sample with Si ion implantation, we could realize a low ohmic contact resistance of $1.5x10^{-5}$ Ωcm^2 led from the CTLM. As a result Si ion implantation technique was very effective to obtain sufficiently low contact resistance to operate the transistor with this AlGaN/AlGaN hetero-structure.

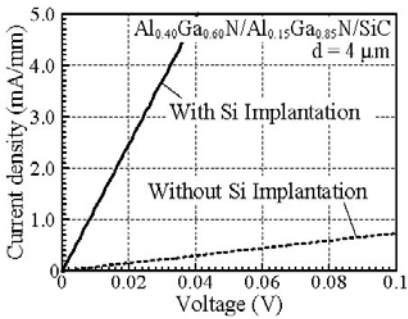

Figure 4. I-V curves between two ohmic electrodes with and without Si ion implantation.

HEMT characteristics

Figure 5 shows a drain current-drain voltage (I_d-V_d) curves measured in dc mode (dashed lines) and pulsed mode (solid lines) in fabricated three HEMTs. The L_g, W_g, L_{sg}, and L_{gd} of the measured HEMTs were 1, 100, 1, and 2 μm, respectively. In all of the HEMTs, we realized transistor operation with good pinch-off characteristics. Although drain current density decreased by the increase of Al composition in epitaxial layers due to the deterioration of electron mobility, maximum values obtained at the gate voltage (V_g) of +2 V were sufficiently high of 0.34 and 0.50 A/mm in the AlGaN channel HEMTs on Sapphire and SiC substrate, respectively. The degradations in the operation of pulsed mode, that is current collapse, were similar in both hetero-structures on the Sapphire substrate. In the AlGaN channel HEMTs on the SiC substrate, however, relatively large current collapse occurred. We consider this current collapse was attributed to residual carriers in the deep region of the channel layer whose possibility will be discussed below.

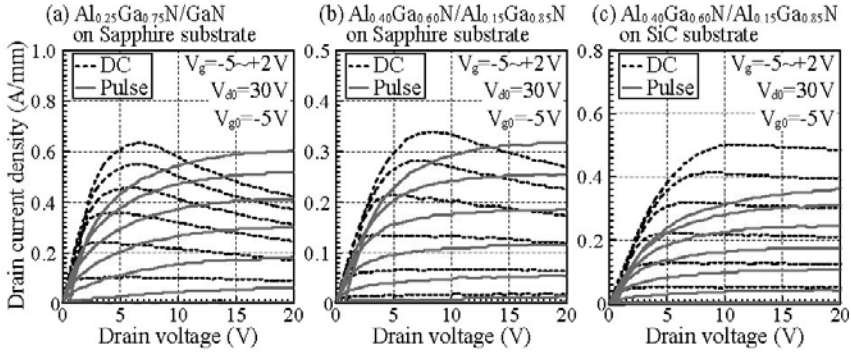

Figure 5. DC and Pulse I_d-V_d curves of (a) $Al_{0.25}Ga_{0.75}N$/GaN HEMT on Sapphire substrate, (b) $Al_{0.40}Ga_{0.60}N/Al_{0.15}Ga_{0.85}N$ HEMT on Sapphire substrate and (c) $Al_{0.40}Ga_{0.60}N/Al_{0.15}Ga_{0.85}N$ HEMT on SiC substrate. The L_g, W_g, L_{sg}, and L_{gd} of the measured HEMTs were 1, 100, 1, and 2 μm, respectively.

By increasing the Al composition in hetero structure, drain breakdown voltage was drastically enhanced. Figure 6 shows V_d dependences of I_d and gate current (I_g) at off-state (V_g = -10 V) in the fabricated three HEMTs with the L_{gd} of 3 and 10 μm, respectively. In the HEMTs with the L_{gd} of 3 μm, which are commonly used for high-frequency devices such as low noise amplifiers, obtained breakdown voltage in AlGaN channel HEMT on Sapphire substrate was 500 V which was higher than that in GaN channel HEMT. In the HEMTs with the L_{gd} of 10 μm, which are commonly used for high-power devices such as switching applications, we realized an extremely high breakdown voltage of 1.7 kV in AlGaN channel HEMT on Sapphire substrate which was much higher than that in GaN channel HEMT. To our knowledge, these are the highest breakdown voltages for group III nitride based HEMTs with similar device dimensions.[2-10] The higher breakdown field due to the wider bandgap contributed to these remarkable breakdown voltage enhancements in AlGaN channel HEMTs. By substituting the substrate to SiC, breakdown voltages decreased regardless of L_{gd} due to the relatively large drain leakage

current in high V_d. Similar drain leakage current had occurred in the AlGaN channel HEMTs using GaN buffer layer on Sapphire substrate and detailed investigation had revealed an existence of residual carriers in the deep region of the channel layer that formed a leakage current pass from source to drain at off-state.[17] We consider, in this study, similar residual carriers existed in the deep region of the channel layer due to the substitution of substrate from Sapphire to SiC, and these residual carriers would also trap electrons in the pulsed mode operation caused current collapse. Although breakdown voltages were decreased, the obtained values were 380 and 1080 V in the HEMTs with the L_{gd} of 3 and 10 μm, respectively, and these were sufficiently higher than that in GaN channel HEMTs.

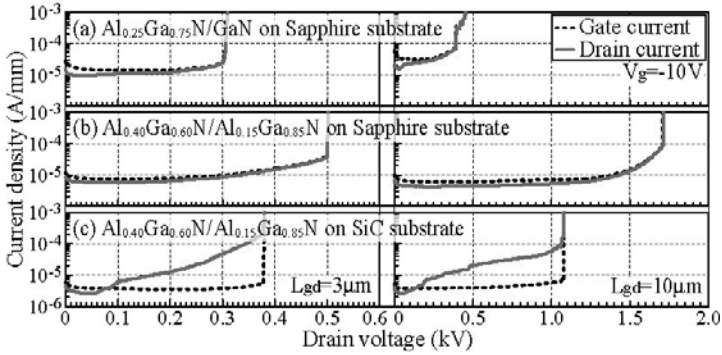

Figure 6. Off-state (V_g = -10 V) I_d-V_d and I_g-V_d curves of (a) $Al_{0.25}Ga_{0.75}N$/GaN HEMT on Sapphire substrate, (b) $Al_{0.40}Ga_{0.60}N/Al_{0.15}Ga_{0.85}N$ HEMT on Sapphire substrate and (c) $Al_{0.40}Ga_{0.60}N/Al_{0.15}Ga_{0.85}N$ HEMT on SiC substrate with the L_{gd} of 3 and 10 μm. The L_g, W_g, and L_{sg} of the measured HEMTs were 1, 100, and 1 μm, respectively.

Finally we compared the obtained specific on-state resistances and breakdown voltages to the state-of-the-art values[3-10] as shown in Fig. 7. These values were obtained in the fabricated three HEMTs with different L_{gd}. We demonstrated that presented AlGaN channel HEMTs were sufficiently competitive to the GaN based devices. We believe that farther development in AlGaN channel HEMTs should realize the high performances exceeding the GaN based devices.

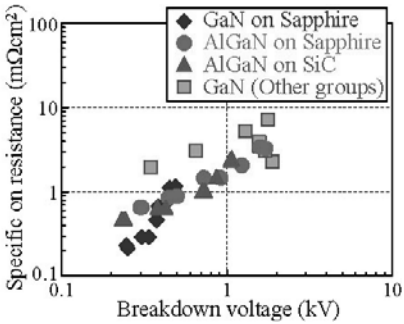

Figure 7. Specific on-state resistances and breakdown voltages in fabricated HEMTs comparing with those in state-of-the-art GaN-based devices.

CONCLUSIONS

Remarkable breakdown voltage enhancements were demonstrated in the AlGaN channel HEMTs. A Si ion implantation doping technique was utilized to reduce an increased ohmic contact resistivity due to applying a high Al mole fractional AlGaN barrier layer. The fabricated AlGaN channel HEMTs with field plate structure demonstrated good pinch-off operation and sufficiently high drain current density over 0.5 A/mm without noticeable current collapse. The obtained breakdown voltage was 1700 V in the AlGaN channel HEMTs with the L_{gd} of 10 μm. These remarkable results indicate that AlGaN channel HEMTs could become future strong candidates for not only high-frequency devices such as low noise amplifiers but also high-power devices such as switching applications.

ACKNOWLEDGMENTS

The authors would like to thank Mr. H. Koyama, Mr. Y. Kamo, and Mr. Y. Nakao for their collaboration in this study.

REFERENCES

1. S. Keller, Y-F. Wu, G. Parish, N. Ziang, J. J. Xu, B. P. Keller, S. P. DenBaars and U. K. Mishra, IEEE Trans. Electron Devices **48**, 552 (2001).
2. T. Kikkawa, Jpn. J. Appl. Phys., Part 1 **44**, 4896 (2005).
3. M. Hikita, M. Yanagihara, K. Nakazawa, H. Ueno, Y. Hirose, T. Ueda, Y. Uemoto, T. Tanaka, D. Ueda and T. Egawa, IEEE Trans. Electron Devices **52**, 1963 (2005)
4. Y. Dora, A. Chakraborty, L. McCarthy, S. Keller, S. P. DenBaars and U. K. Mishra, IEEE Electron Device Lett. **27**, 713 (2006)

5. N. Tipirneni. A. Koudymov, V. Adivarahan, J. Yang, G. Simin and M. A. Khan, IEEE Electron Device Lett. **27**, 716 (2006)
6. C. S. Suh, Y. Dora, N. Fichtenbaum, L. McCarthy, S. Keller, and U. K. Mishra, Tech. Dig. - Int. Electron Devices Meet. (2006).
7. Y. C. Choi, J. Shi, M. Pophristic, M. G. Spencer and L. F. Eastman, J. Vac. Sci. Technol. B **25**, 1836 (2007)
8. Y. Uemoto, D. Shibata, M. Yanagihara, H. Ishida, H. Matsuo, S. Nagai, N. Batta, M. Li, T. Ueda, T. Tanaka, and D. Ueda, Tech. Dig. - Int. Electron Devices Meet. (2007).
9. T. Morita, M. Yanagihara, H. Ishida, M. Hikita, K. Kaibara, H. Matsuo, Y. Uemoto, T. Ueda, T. Tanaka and D. Ueda, Tech. Dig. - Int. Electron Devices Meet. (2007).
10. N. Ikeda, Y. Niiyama. H. Kambayashi, Y. Sato, T. Nomura, S. Kato and S. Yoshida, Proc. IEEE, **98**, 1151 (2010)
11. M. Suita, T. Nanjo, T. Oishi, Y. Abe and Y. Tokuda, Phys. Status Solidi C **3**, 2364 (2006)
12. T. Oishi, N. Miura, M. Suita, T. Nanjo, Y. Abe, and T. Ozeki, H. Ishikawa, T. Egawa and T. Jimbo, J. Appl. Phys. **94**, 1662 (2003).
13. Y. Kamo, T. Kunii H. Takeuchi, Y. Yamamoto, M. Totsuka, T. Shiga, H. Minami, T. Kitano, S. Miyakuni, T. Oku, A. Inoue, T. Nanjo, Y. Tsuyama, R. Shirahana, K. Iyomasa, K. Yamanaka, T. Ishikawa, T. Takagi, K. Marumoto and Y. Matsuda, 2005 IEEE MTT-S Int. Microwave Symp. Dig. **495** (2005).
14. M. Higashiwaki, N. Hirose and T. Matsui: IEEE Electron Device Lett. **26, 139** (2005).
15. M. Higashiwaki, T. Matsui and T. Mimura: IEEE Electron Device Lett. **27,** 16 (2006).
16. A. Raman, S. Dasgupta, S. Rajan, J. S. Speck and U. K. Mishra, Jpn. J. Appl. Phys., **47**, 3357 (2008)
17. T. Nanjo, M. Takeuchi, A. Imai, M. Suita, T. Oishi, Y. Abe, E. Yagyu, T. Kurata, Y. Tokuda and Y. Aoyagi, Electron. Lett. **39**, 750 (2003).